ORGANIC LETTERS

2011
Vol. 13, No. 8
2130–2133

Tandem Phospha-Friedel–Crafts Reaction toward Curved π-Conjugated Frameworks with a Phosphorus Ring Junction

Takuji Hatakeyama,*,† Sigma Hashimoto,†,‡ and Masaharu Nakamura*,†

International Research Center for Elements Science, Institute for Chemical Research, and Department of Energy and Hydrocarbon Chemistry, Graduate School of Engineering, Kyoto University, Uji, Kyoto, 611-0011, Japan

hatake@scl.kyoto-u.ac.jp; masaharu@scl.kyoto-u.ac.jp

Received March 6, 2011

ABSTRACT

The tandem phospha-Friedel–Crafts reaction transforms dichloro(*m*-teraryl)phosphine to the corresponding triarylphosphine derivatives containing curved π-conjugated frameworks with a phosphorus ring junction. The rigid molecular frameworks enable these unprecedented phosphine compounds to hold an extended π-conjugation spread over the whole molecule.

π-Conjugated molecules are an important class of materials for organic electronics, dyes, sensors, and liquid crystals.[1] Incorporation of heteroatoms into a π-conjugated skeleton is a promising way to modulate their physical properties, and thus, intensive efforts have been devoted to the construction of new hetero-π-conjugated frameworks.[2] Because of the lack of a suitable synthetic method, only a few π-conjugated molecules with ring junction heteroatoms[3,4] have been synthesized to date, even though numerous theoretical investigations[5] suggested that those hetero-π-conjugated molecules could be attractive substructures of heteroatom-embedded nanocarbons.[6] We envisioned that the development of a *tandem* hetero Friedel–Crafts reaction[7] could provide facile access to the π-conjugated frameworks with ring junction heteroatoms as shown in Scheme 1. To avoid undesirable five-member-ring formation established as the heterole synthesis,[7c,d,f–h] we have done careful screening of additives, reaction conditions, and

† International Research Center for Elements Science, Institute for Chemical Research.

‡ Department of Energy and Hydrocarbon Chemistry.

(1) Reviews: (a) Fabian, J.; Nakazumi, H.; Matsuoka, M. *Chem. Rev.* **1992**, *92*, 1197–1226. (b) Scherf, U. *J. Mater. Chem.* **1999**, *9*, 1853–1864. (c) Mitschke, U.; Bäuerle, P. *J. Mater. Chem.* **2000**, *10*, 1471–1507. (d) Watson, M. D.; Fechtenkötter, A.; Müllen, K. *Chem. Rev.* **2001**, *101*, 1267–1300. (e) Bendikov, M.; Wudl, F.; Perepichka, D. F. *Chem. Rev.* **2004**, *104*, 4891–4945. (f) Klauk, H. *Organic Electronics*; Wiley-VCH: Weinheim, 2006. (g) Anthony, J. E. *Chem. Rev.* **2006**, *106*, 5028–5048. (h) Sergeyev, S.; Pisula, W.; Geerts, Y. H. *Chem. Soc. Rev.* **2007**, *36*, 1902–1929. (i) Wu, J.; Pisula, W.; Müllen, K. *Chem. Rev.* **2007**, *107*, 718–747.

(2) Reviews: (a) Yamaguchi, S.; Xu, C.; Okamoto, T. *Pure Appl. Chem.* **2006**, *78*, 721–730. (b) Yamaguchi, S.; Wakamiya, A. *Pure Appl. Chem.* **2006**, *78*, 1413–1324. (c) Baumgartner, T.; Réau, R. *Chem. Rev.* **2006**, *106*, 4681–4727. (d) Loudet, A.; Burgess, K. *Chem. Rev.* **2007**, *107*, 4891–4932. (e) Fukazawa, A.; Yamaguchi, S. *Chem.—Asian J.* **2009**, *4*, 1386–1400. (f) Matano, Y.; Imahori, H. *Org. Biomol. Chem.* **2009**, *7*, 1258–1271.

(3) (a) Leupin, W.; Wirz, J. *J. Am. Chem. Soc.* **1980**, *102*, 6068–6075. (b) Takase, M.; Enkelmann, V.; Sebastiani, D.; Baumgarten, M.; Müllen, K. *Angew. Chem., Int. Ed.* **2007**, *46*, 5524–5527. (c) Wu, D.; Pisula, W.; Enkelmann, V.; Feng, X.; Müllen, K. *J. Am. Chem. Soc.* **2009**, *131*, 9620–9621. (d) Wharton, S. I.; Henry, J. B.; MacNab, H.; Mount, A. R. *Chem.—Eur. J.* **2009**, *15*, 5482–5490.

(4) The substitution of B–N fragments for C–C fragments in aromatic hydrocarbons has been well investigated: Bosdet, M. J. D.; Piers, W. E. *Can. J. Chem.* **2008**, *86*, 8–29 and references cited therein.

(5) Selected papers: (a) Casanovas, J.; Ricart, J. M.; Rubio, J.; Illas, F.; Jiménez-Mateos, J. M. *J. Am. Chem. Soc.* **1996**, *118*, 8071–8076. (b) Kurita, N.; Endo, M. *Carbon* **2002**, *40*, 253–260. (c) Tran, F.; Alameddine, B.; Jenny, T. A.; Wesolowski, T. A. *J. Phys. Chem. A* **2004**, *108*, 9155–9160. (d) Hasegawa, T.; Suzuki, T.; Mukai, S. R.; Tamon, H. *Carbon* **2004**, *42*, 2195–2200. (e) Mandumpal, J.; Gemming, S.; Seifert, G. *Chem. Phys. Lett.* **2007**, *447*, 115–120.

(6) Reviews: (a) Kawaguchi, M. *Adv. Mater.* **1997**, *9*, 615–625. (b) Terrones, M.; Jorio, A.; Endo, M.; Rao, A. M.; Kim, Y. A.; Hayashi, T.; Terrones, H.; Charlier, J.-C.; Dresselhaus, G.; Dresselhaus, M. S. *Mater. Today* **2004**, *7*, 30–45. (c) Vostrowsky, O.; Hirsch, A. *Chem. Rev.* **2006**, *106*, 5191–5207.

10.1021/ol200571s © 2011 American Chemical Society
Published on Web 03/24/2011

Scheme 1. *Tandem* Hetero Friedel–Crafts Reaction toward a π-Conjugated Framework

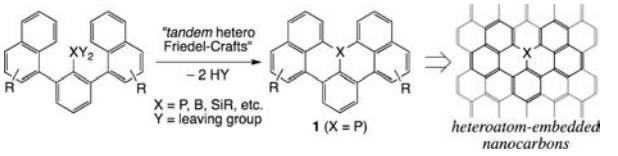

starting substrates. Finally, we have found that the *tandem* phospha-Friedel–Crafts reaction of dichloro(*m*-teraryl)-phosphine (XY_2 = PCl_2) affords phosphaperylenes **1** via selective 6,6-ring-closure under particular conditions. Herein, we disclose experimental details of the synthesis, crystal structures, and physical properties of **1** and their derivatives.

Scheme 2. Synthesis of **1**–**5**

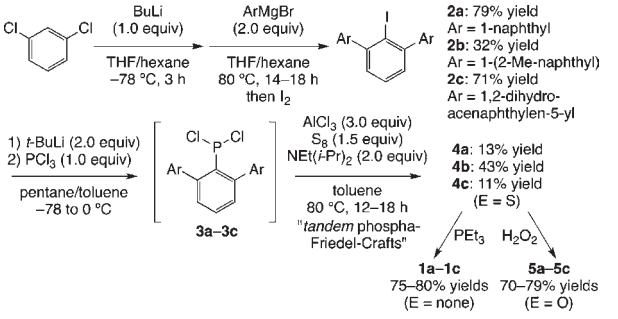

The synthetic route is described in Scheme 2: selective lithiation at the 2-position of 1,3-dichlorobenzene and subsequent treatment with 2 equiv of aryl Grignard reagents gave *m*-teraryl iodides **2a**–**2c** in 32–79% yields upon iodination quenching.[8] Lithium–halogen exchange of **2a**–**2c** and subsequent trapping of the resulting aryllithiums with trichlorophosphine gave *m*-terarylphosphine dichlorides **3a**–**3c**. After the careful screening of additives and reaction conditions, the tandem phospha-Friedel–Crafts reaction of **3a**–**3c** was achieved by the combined use of S_8, $AlCl_3$, and NEt(*i*-Pr)$_2$.[9] Notably, the tandem reaction selectively gave 6,6-ring-closure products, phosphine sulfides **4a**–**4c** (E = S), in 11–43% yields, and no formation of 5,5- or 5,6-ring-closure products was observed under the present reaction conditions.

(7) Nontandem reactions have been reported. Phosphorus: (a) Olah, G. A.; Hehemann, D. *J. Org. Chem.* **1977**, *42*, 2190. (b) Wang, Z.-W.; Wang, L.-S. *Green Chem.* **2003**, *5*, 737–739. (c) Diaz, A. A.; Young, J. D.; Khan, M. A.; Wehmschulte, R. J. *Inorg. Chem.* **2006**, *45*, 5568–5575. (d) Diaz, A. A.; Buster, B.; Schomich, D.; Khan, M. A.; Baum, J. C.; Wehmschulte, R. J. *Inorg. Chem.* **2008**, *47*, 2858–2863. Silicon: (e) Olah, G. A.; Bach, T.; Prakash, G. K. S. *J. Org. Chem.* **1989**, *54*, 3770–3771. (f) Furukawa, S.; Kobayashi, J.; Kawashima, T. *J. Am. Chem. Soc.* **2009**, *131*, 14192–14193. Boron: (g) Genaev, A. M.; Nagy, S. M.; Salnikov, G. E.; Shubin, V. G. *Chem. Commun.* **2000**, 1587–1588. (h) Vries, T. S. D.; Prokofjevs, A.; Harvey, J. N.; Vedejs, E. *J. Am. Chem. Soc.* **2009**, *131*, 14679–14687.

(8) (a) Du, C.-J. F.; Hart, H.; Ng, K.-K. D. *J. Org. Chem.* **1986**, *51*, 3162–3165. (b) Saednya, A.; Hart, H. *Synthesis* **1996**, 1455–1458.

(9) The reaction did not proceed at all in the absence of S_8. The reaction gave several byproducts in the absence of NEt(*i*-Pr)$_2$.

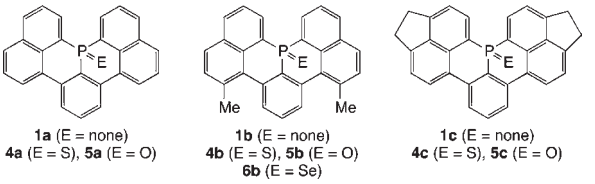

Figure 1. Phosphaperylene derivatives.

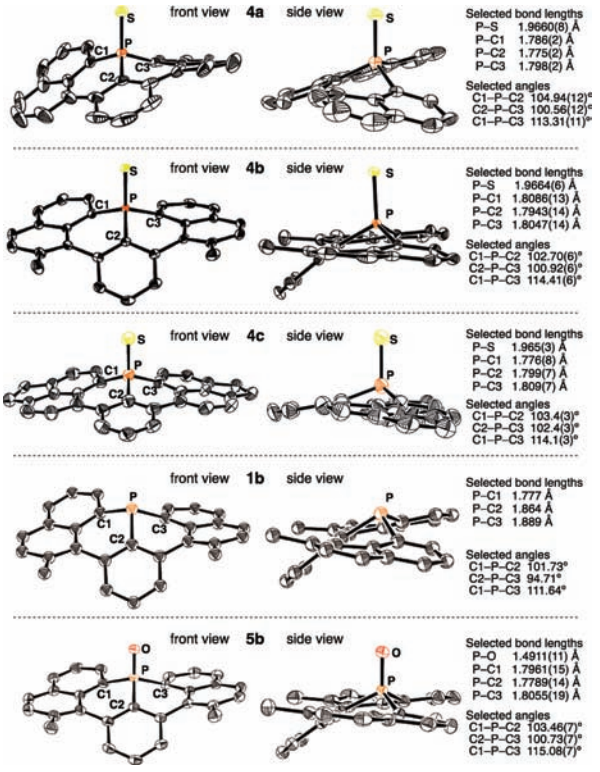

Figure 2. ORTEP drawings of (*M*)-**4a**–**4c**, (*M*)-**1b**, and (*M*)-**5b**. Thermal ellipsoids are shown at 50% probability except for **1b**;[10] hydrogen atoms have been omitted for clarity.

Desulfurization of **4a**–**4c** with triethylphosphine gave the target phosphines, 15b-phosphanaphtho[1,8-*ab*]perylene **1a**, 6,10-dimethyl-15b-phosphanaphtho[1,8-*ab*]perylene **1b**, and 15b-phospha-3,4,12,13-tetrahydroacenaphtho[5,6-*ab*]cyclopenta[*lm*]perylene **1c**, in 75–80% yields. Similarly, oxidation with H_2O_2 gave the corresponding phosphine oxides **5a**–**5c** in 70–79% yields (Figure 1).

The structures of phosphine sulfides **4a**–**4c**, phosphine **1b**, and phosphine oxide **5b** were determined by X-ray crystallography (Figure 2).[10] The phosphorus centers adopt a distorted tetrahedral geometry with C–P–C bond angles of 100.56(12)°–113.31(11)°, 100.92(6)°–114.41(7)°, 102.4

(10) The structure of **1b** was determined by Rietveld refinement from X-ray powder diffraction data without any atomic displacement parameters. See the Supporting Information for details of the X-ray crystallography.

(3)°−114.1(3)°, 94.71°−111.64°, and 100.73(7)°−115.08(7)°, respectively. In line with the tetrahedral geometry of the phosphorus centers as well as steric repulsion between the hydrogen atoms at the β-position of the phosphorus atom, **4a** adopts a helical structure (the *M*-enantiomer is shown). On the other hand, **4b** adopts a bowl-shaped structure because of steric repulsion between the methyl groups and the phenyl group. Interestingly, **4c** adopts a planar structure rather than a helical structure.[11] Phosphine **1b** and phosphine oxide **5b** show an analogous structure to phosphine sulfide **4b**. Note that these phosphaperylene derivatives are thermally stable: none of the derivatives decompose below 600 K.

Molecular orbital calculations of the phosphines and their derivatives[12] indicate extended π-conjugation spread over the whole molecule despite the curved structures: the HOMO and LUMO of **1a** and **5a** delocalize on the whole molecular surface (Figure 3). The HOMO−LUMO gaps of **1a** (3.60 eV) and **5a** (3.68 eV) are comparable to that of anthracene (3.59 eV). Note that the HOMO of **1a** consists of the p-orbital of the phosphorus atom and aromatic π-orbitals. The HOMO and LUMO energies of **5a** are lower than those of **1a** (0.43 and 0.51 eV, respectively) because of the electron-withdrawing nature of the P═O group.

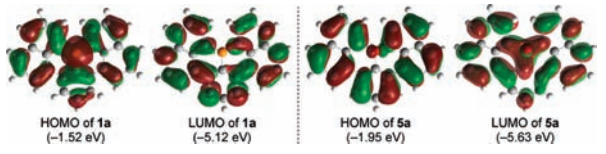

Figure 3. Kohn−Sham HOMO and LUMO of **1a** and **5a**.

Table 1 summarizes the photophysical properties of phosphines **1a** and **1b** and phosphine oxides **5a**−**5c**. In the UV/vis absorption spectra, phosphines and phosphine oxides have a strong absorption band with a maximum (λ_{abs}) at 379−412 nm, which is assignable to an HOMO−LUMO transition by the TD-DFT calculations.[13] Smaller absorption coefficients of phosphines **1a** and **1b** (log ε = 3.63 and 3.20, respectively) than those of phosphine oxides **5a** and **5b** (log ε = 4.13 and 4.11, respectively) are consistent with smaller oscillator strengths for the HOMO−LUMO transition calculated by the TD-DFT method, which can be explained by a substantial contribution of the p-orbital of the phosphorus atom to the HOMO but not to the LUMO as shown in Figure 2. Phosphine **1a** exhibits a strong green fluorescence with two peaks, one at 436 nm and a broader excimer-type emission at 540 nm. A similar excimer-type emission[14] was also observed in the fluorescence spectrum of phosphine **1b**.[15] Phosphine oxides **5a**, **5b**, and **5c** exhibit strong blue and cyan fluorescences with a maximum (λ_{em}) at 418, 415, and 468 nm, respectively. The quantum yield of **5b** (Φ_f = 0.83) is larger than that of **5a** (Φ_f = 0.68). A comparable radiative rate constant (k_r, 3.0×10^8 vs 4.0×10^8 s^{-1}) and a smaller nonradiative rate constant for **5b** (k_{nr}, 6.2×10^9 vs 1.9×10^8 s^{-1}) indicate that the methyl substituents would kinetically stabilize the conformation to suppress the nonradiative decay process. On the other hand, **5c** shows a lower fluorescence efficiency of Φ_f = 0.20 with a smaller radiative rate constant (k_r, 3.9×10^7 s^{-1}) and a comparable nonradiative rate constant (k_{nr}, 1.6×10^8 s^{-1}).

Table 1. Photophysical Data and HOMO−LUMO Transition Calculated by the TD-DFT Method for **1a**−**b** and **5a**−**5c**

	UV−vis absorption[a]		fluorescence[a]				calculated transition[b]	
compd	λ_{abs}[c] (nm)	log ε	λ_{em}[d] (nm)	Φ_f[e]	τ_s[f] (ns)	k_r/k_{nr}[g] (10^8 s^{-1})	λ_{em} (nm)	ocillator strength
1a	407	3.63	436, 540	–	–	–	417	0.1621
1b	400	3.20	428, 505	–	–	–	397	0.1564
5a	388	4.13	418	0.68	1.72	4.0/1.9	392	0.2443
5b	379	4.11	415	0.83	2.74	3.0/0.62	387	0.2624
5c	412	3.90	468	0.20	5.11	0.39/1.6	410	0.2708

[a] UV/vis absorption and fluorescence measurements were made in CH_2Cl_2 (0.02 and 0.01 mM, respectively). [b] Only the lowest-energy (HOMO−LUMO) transitions calculated by the TD-DFT method are shown. [c] Only the longest absorption maxima are shown. [d] Emission maxima upon excitation at 360 nm (**5a**−**5c**) and 400 nm (**1a** and **1b**). [e] Absolute fluorescence quantum yields determined by a calibrated integrating sphere system with ≤3% errors. [f] Fluorescence lifetime. [g] The radiative rate constant (k_r) and nonradiative rate constant (k_{nr}) were calculated from Φ_f and τ_s using the formula $k_r = \Phi_f/\tau_s$ and $k_{nr} = (1 - \Phi_f)/\tau_s$.

Phosphine selenide **6b** (E = Se) prepared from phosphine **1b** shows a relatively small $^1J_{P-Se}$ coupling constant (687 Hz), which indicates a high p-orbital contribution of the P═Se bond (cf. Ph_3P═Se: 732 Hz, $^tBu_3P$═Se: 686 Hz).[16] The coordination ability of **1b** has been demonstrated by efficient formation (97% yield) of a 1:1 complex with AuCl (Figure 4a). The X-ray crystal structure shows a P−Au distance of 2.2343(12) Å (Figure 4b), which is comparable with those of $AuCl(PPh_3)$ and $AuCl(P^tBu_3)$ (2.233 and 2.253 Å, respectively).[17] The novel π-conjugated phosphines may offer potential utility not only as a material but also as a ligand for transition metal catalysis.

In summary, we have developed a tandem intramolecular phospha-Friedel−Crafts reaction to synthesize curved π-conjugated molecules with a phosphorus ring junction. In

(11) All of these derivatives have helical chirality to some degree and formed racemic crystals.

(12) The DFT calculations were performed using the B3LYP hybrid functional with the 6-31G(d) basis set. See the Supporting Information for other derivatives and other orbitals.

(13) The TD-DFT calculations were performed for **1a**−**b** and **5a**−**c** at the B3LYP/6-311+G(d,p) level based on the optimized structures at the B3LYP/6-31G(d) level. See the Supporting Information for details.

(14) The relative intensity of the emission at 505 nm to the emission at 428 nm increases in proportion to the concentration of **1b**. See the Supporting Information for details.

(15) Absolute fluorescence quantum yields (F_f) of **1a** and **1b** have not been determined because partial in situ P-oxidation during the measurements introduces errors.

(16) $^1J_{P-Se}$ coupling constants measured in $CDCl_3$: (a) Allen, D. W.; Taylor, B. F. *J. Chem. Soc., Dalton Trans.* **1982**, 51–54. (b) Ohta, H.; Tokunaga, M.; Obora, Y.; Iwai, T.; Iwasawa, T.; Fujihara, T.; Tsuji, Y. *Org. Lett.* **2007**, *9*, 89–92.

(17) (a) Banditelli, G.; Bandini, A. L.; Minghetti, G.; Bonati, F. *Can. J. Chem.* **1981**, *59*, 1241–1246. (b) Schmidbaur, H.; Brachthäuser, B.; Steigelmann, O.; Beruda, H. *Chem. Ber.* **1992**, *125*, 2705–2710.

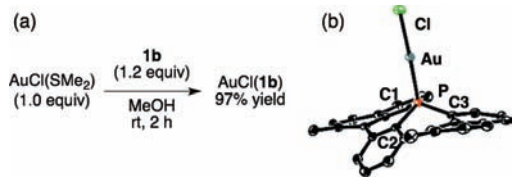

Figure 4. (a) Preparation and (b) ORTEP drawing of (*M*)-AuCl(**1b**). Selected bond lengths (Å) and angle (deg): Au−Cl 2.2945(12), Au−P 2.2343(12), P−C1 1.805(6), P−C2 1.786(5), P−C3 1.815(6), P−Au−Cl 175.13(6).

line with the tetrahedral geometry of the phosphorus centers as well as steric demands of the substituents, the π-conjugated molecules adopt helical, bowed, and planar structures. The rigid molecular frameworks enable these unprecedented phosphine compounds to hold a π-conjugation spread over the whole molecule. This simple and practical strategy would be suitable for further extension of π-conjugated frameworks as well as the introduction of multiple phosphorus and/or other heteroatoms.

Acknowledgment. This work was partially supported by a Grant-in-Aid for Scientific Research on Innovative Areas "Integrated Organic Synthesis" (T.H., 22106524), a Grant-in-Aid for Young Scientists (S, M.N., 20675003), and Research for Promoting Technological Seeds (T.H., 1102) from JSPS and MEXT. We truly appreciate the fluorescence measurements by Professor Masaki Shimizu (Kyoto University). We gratefully acknowledge Professors Hikaru Takaya (Kyoto University), Takahiro Sasamori (Kyoto University), and Yoshiyuki Mizuhata (Kyoto University) for their experimental help and guidance on X-ray crystallography and Professor Atsushi Wakamiya (Kyoto University) for helpful discussions on photophysical data. Professor Norihiro Tokitoh (Kyoto University) is also acknowledged for generous permission to use an X-ray diffractometer. We also thank Mr. Tsuyoshi Oba (Kyoto University) for his experimental support. The synchrotron X-ray powder diffraction measurement was performed at the BL19B2 in the SPring-8 with the approval of JASRI (T.H., 2009B1785).

Supporting Information Available. Experimental procedure, characterization, photophysical data, crystallographic data, and CIF files for the products (PDF), as well as computational method and data. This material is available free of charge via the Internet at http://pubs.acs.org.